



## Calculations of NMR chemical shifts with APW-based methods

Robert Laskowski and Peter Blaha

*Institute of Materials Chemistry, Vienna University of Technology, Getreidemarkt 9/165TC, AT-1060 Vienna, Austria*

(Received 21 December 2011; published 31 January 2012)

We present a full potential, all electron augmented plane wave (APW) implementation of first-principles calculations of NMR chemical shifts. In order to obtain the induced current we follow a perturbation approach [Pickard and Mauri, *Phys. Rev. B* **63**, 245101 (2001)] and extended the common APW + local orbital (LO) basis by several LOs at higher energies. The calculated all-electron current is represented in traditional APW manner as Fourier series in the interstitial region and with a spherical harmonics representation inside the nonoverlapping atomic spheres. The current is integrated using a “pseudocharge” technique. The implementation is validated by comparison of the computed chemical shifts with some “exact” results for spherical atoms and for a set of solids and molecules with available published data.

DOI: [10.1103/PhysRevB.85.035132](https://doi.org/10.1103/PhysRevB.85.035132)

PACS number(s): 71.45.Gm, 76.60.Cq, 71.15.–m

### I. INTRODUCTION

Nuclear magnetic resonance (NMR) is a widely used experimental technique in structural chemistry.<sup>1</sup> It measures a fundamental property of any material, namely, its response to an external magnetic field. An external magnetic field  $\mathbf{B}$  induces an electric current  $\mathbf{j}_{\text{ind}}$  in the sample and this current is the source of an induced magnetic field  $\mathbf{B}_{\text{ind}}$ . NMR experiments measure the induced field at the nucleus by measuring the transition energies related to the reorientation of the nuclear magnetic moment. Because the induced current and therefore the induced field depends strongly on the atomic and electronic structure of the investigated material, the NMR measurements provide an information about these properties. Nowadays, NMR is routinely used for studying the structures of molecules and solids. In the case of molecules, the interpretation of the measured spectra is often based on a set of empirical rules that capture the indirect relation between the atomic structure and the NMR spectra.<sup>2</sup> However, for some systems, the response depends on the details of the electronic structure, which makes the interpretation of experimental data rather difficult. At this point *ab initio* calculations became extremely helpful in assigning the chemical shifts to specific sites. This is especially true for solids, where empirical rules are much more difficult to develop.<sup>3</sup>

Until now several methods of *ab initio* calculation of NMR chemical shifts for molecules<sup>4,5</sup> and solids have been described in the literature.<sup>6–10</sup> At least for solids, they solve the electronic structure within density functional theory (DFT)<sup>11,12</sup> and most of them use a perturbative approach to construct the response current, which is then integrated utilizing the Biot-Savart law to calculate the induced magnetic fields at the nuclei and the corresponding magnetic shielding factors  $\sigma$ . The task of computing the induced current is complicated by the fact that the magnetic field breaks translational symmetry. Moreover, the position operator, which explicitly enters the perturbed Hamiltonian, is not well defined for extended systems. The first method that overcomes this difficulty, was proposed by Mauri, Pfrommer, and Louie (MPL), where the external magnetic field is modulated with a finite wave vector.<sup>6</sup> The response is calculated taking the limit at infinite length of the modulation vector. It can be shown that for finite systems

the MPL method is equivalent to a variant of the continuous set of gauge transformations (CSGT) method.<sup>13</sup> The MPL method has been derived and implemented for plane-wave based pseudopotential codes, however, it neglects the effects of the pseudoization of the wave functions on the induced current, which should be considerable in the core region of heavier atoms. Despite of this fact, it has been used in several interesting applications, but limited to light elements and with the use of hard pseudopotentials.<sup>14–19</sup> This drawback has been removed by Pickard and Mauri.<sup>8</sup> Their approach operates within the projector augmented-wave method (PAW)<sup>20</sup> and defined the PAW transformations such that they ensure correct gauge (translational) symmetry of the pseudo-wave-function in the presence of the external magnetic field. Due to this new form, the method is referred in literature as gauge-including projector augmented-wave (GIPAW) method. Furthermore, the GIPAW approach has been reformulated such that it can be based on ultrasoft-pseudopotential calculations.<sup>21</sup> The method has been shown to be very useful and numerous applications covering a broad spectrum of materials from minerals<sup>22–26</sup> to molecular crystals<sup>27–29</sup> have been published. An extensive list of applications can be found at Ref. 30. Another approach, proposed by Sebastiani and Parrinello exploits the exponentially decaying character of localized Wannier orbitals combined with a saw-shaped “periodized” position operator,<sup>7</sup> such that the discontinuity due to the periodization appears in a region where the Wannier functions vanish. The main advantage of this method is that for large systems it requires considerably lower computational efforts than MPL or GIPAW. Therefore, it is easier to apply this method to problems that require large unit cells such as *ab initio* molecular dynamics simulations of biological systems.<sup>31</sup> This approach has been implemented not only in pure plane-wave based codes, but also in an all-electron Gaussian and augmented-plane-wave method (GAPW).<sup>32,33</sup> Recently, a “converse” approach, that does not rely on perturbation theory has been introduced.<sup>9,34</sup> In this case, the shielding tensor is obtained from the derivative of the orbital magnetization with respect to the application of a localized magnetic dipole. In order to calculate the necessary magnetization, the ground-state problem with an additional term in the Hamiltonian describing the potential generated by the localized dipole, has to be solved. This usually requires

a supercell approach to ensure a proper separation of the localized dipoles.

In the present paper, we describe the formalism of NMR chemical shift calculations for the full-potential all-electron linear augmented-plane-wave (LAPW) method.<sup>35</sup> The actual implementation has been realized in the WIEN2k code.<sup>36</sup> In this method, we do not impose any restriction or approximation to the induced current density. Also the integration of the all-electron current is performed without further approximations. The paper is organized as follows. In order to keep the presentation self-contained, we shortly discuss in the next section the application of the DFT perturbation theory for the computation of the induced current density in the presence of a uniform external magnetic field. Next, the details related to the specific form of the LAPW basis are presented, focusing on the integration of the induced all-electron current, as this is inherently different from the one applied in the pseudopotential codes. In Sec. III, we test our implementation, focusing on the basis set quality by showing that our method is able to reproduce the diamagnetic response of isolated atoms. Section IV contains the final validation of the method by comparing the calculated shielding for several solids and molecules with the available published data.

## II. IMPLEMENTATION DETAILS

### A. Induced current in DFT perturbation theory

For a small external magnetic field, a linear relation between the induced and external field holds:

$$\mathbf{B}_{\text{ind}}(\mathbf{R}) = -\overleftrightarrow{\sigma}(R)\mathbf{B}, \quad (1)$$

where  $\overleftrightarrow{\sigma}$  is the absolute chemical shift tensor. In order to calculate the  $\mathbf{B}_{\text{ind}}$  field induced by the external field  $\mathbf{B}$ , we apply the Biot-Savart law:

$$\mathbf{B}_{\text{ind}}(\mathbf{R}) = \frac{1}{c} \int d^3r \mathbf{j}_{\text{ind}}(\mathbf{r}) \times \frac{\mathbf{R} - \mathbf{r}}{|\mathbf{r} - \mathbf{R}|^3}, \quad (2)$$

where the induced current density  $\mathbf{j}_{\text{ind}}(\mathbf{r})$  is the key component. In the case of nonmagnetic and insulating materials, only the orbital motion of the electrons is affected by the magnetic field and contributes to the induced current  $\mathbf{j}_{\text{ind}}(\mathbf{r})$ . The single-particle Hamiltonian in the presence of the magnetic field takes the following form:

$$H = \frac{1}{2} \left[ \mathbf{p} + \frac{1}{c} \mathbf{A}(\mathbf{r}) \right]^2 + V(\mathbf{r}), \quad (3)$$

where  $\mathbf{p}$  is the momentum operator,  $V(\mathbf{r})$  is the effective single-particle potential, and  $\mathbf{A}(\mathbf{r})$  is the vector potential related to the external magnetic field with  $\mathbf{B} = \nabla \times \mathbf{A}(\mathbf{r})$ . In the symmetric gauge,  $\mathbf{A}(\mathbf{r}) = \frac{1}{2} \mathbf{B} \times \mathbf{r}$  and the Hamiltonian becomes

$$H = \frac{1}{2} \mathbf{p}^2 + V(\mathbf{r}) + \frac{1}{2c} \mathbf{r} \times \mathbf{p} \cdot \mathbf{B} + \frac{1}{8c^2} (\mathbf{B} \times \mathbf{r})^2, \quad (4)$$

where the first two terms constitute the unperturbed Hamiltonian, and the third term is the first-order perturbation [ $H^{(1)}$ ] with respect to the external field  $\mathbf{B}$ :

$$H^{(1)} = \frac{1}{2c} \mathbf{r} \times \mathbf{p} \cdot \mathbf{B}. \quad (5)$$

The induced current density  $\mathbf{j}_{\text{ind}}$  is calculated as first-order variation of the expectation value of the current operator with respect to the external field  $\mathbf{B}$ . The current operator in the presence of the magnetic field in the chosen gauge has the following form:

$$\mathbf{J}(\mathbf{r}') = \mathbf{J}^p(\mathbf{r}') + \mathbf{J}^d(\mathbf{r}'), \quad (6)$$

$$\mathbf{J}^p(\mathbf{r}') = -\frac{\mathbf{p}|\mathbf{r}'\rangle\langle\mathbf{r}'| + |\mathbf{r}'\rangle\langle\mathbf{r}'|\mathbf{p}}{2}, \quad (7)$$

$$\mathbf{J}^d(\mathbf{r}') = -\frac{\mathbf{B} \times \mathbf{r}'}{2c} |\mathbf{r}'\rangle\langle\mathbf{r}'|, \quad (8)$$

where  $\mathbf{J}^p$  and  $\mathbf{J}^d$  are the paramagnetic and diamagnetic current operators. The form of the diamagnetic operator is strictly related to the chosen gauge. Therefore partitioning of the total current into paramagnetic and diamagnetic contributions does not have a fundamental meaning. Within density functional theory, the total current density is evaluated as a sum of expectation values of the current operator applied to the occupied Kohn-Sham states. Because our goal is to calculate the induced current, the sum will involve only the first-order terms with respect to the external field:

$$\mathbf{j}_{\text{ind}}(\mathbf{r}') = \sum_o [\langle \Psi_o^{(1)} | \mathbf{J}^{(0)}(\mathbf{r}') | \Psi_o^{(0)} \rangle + \langle \Psi_o^{(0)} | \mathbf{J}^{(0)}(\mathbf{r}') | \Psi_o^{(1)} \rangle + \langle \Psi_o^{(0)} | \mathbf{J}^{(1)}(\mathbf{r}') | \Psi_o^{(0)} \rangle], \quad (9)$$

where  $\Psi_o^{(0)}$  represents an occupied orbital of the unperturbed Hamiltonian.  $J^0(\mathbf{r}')$  is the unperturbed part of the current operator and equal to the paramagnetic current operator.  $J^1(\mathbf{r}')$  is the first-order perturbation of the current and corresponds to the diamagnetic current operator.  $\Psi_o^{(1)}$  is the first-order perturbation of  $\Psi_o^{(0)}$ , projected on the subspace of the unoccupied states. It is evaluated using the standard perturbation theory formula

$$|\Psi_o^{(1)}\rangle = \mathcal{G}(\epsilon_o) H^{(1)} |\Psi_o^{(0)}\rangle, \quad (10)$$

where  $\mathcal{G}$  is the Green function operator:

$$\mathcal{G}(\epsilon) = \sum_e \frac{|\Psi_e^{(0)}\rangle\langle\Psi_e^{(0)}|}{\epsilon - \epsilon_e}, \quad (11)$$

and the sum is running over the empty (unoccupied) Kohn-Sham orbitals. Including expressions for  $J^0(\mathbf{r}')$ ,  $J^1(\mathbf{r}')$ , and  $\Psi_o^{(1)}$  into Eq. (9), we obtain

$$\mathbf{j}_{\text{ind}}(\mathbf{r}') = \sum_o \text{Re} [\langle \Psi_o^{(0)} | \mathbf{J}^p(\mathbf{r}') \mathcal{G}(\epsilon_o) H^{(1)} | \Psi_o^{(0)} \rangle ] - \frac{1}{2c} \rho(\mathbf{r}') \mathbf{B} \times \mathbf{r}'. \quad (12)$$

The first and second terms in this formula represent the paramagnetic and diamagnetic current contributions to the total induced current. These terms individually depend on the gauge origin, or in the symmetric gauge, on the choice of the origin of the unit cell and they may become large and opposite in sign. This represents a problem for practical calculations where finite basis sets are used for computing the unperturbed wave functions. In order to avoid such convergence problems, it

is convenient to rewrite the diamagnetic contribution using a commutator:

$$\rho(\mathbf{r}')\mathbf{B} \times \mathbf{r}' = - \sum_o \langle \Psi_o^{(0)} | \frac{1}{i} [\mathbf{B} \times \mathbf{r}' \cdot \mathbf{r}, \mathbf{J}^p(\mathbf{r}')] | \Psi_o^{(0)} \rangle. \quad (13)$$

After employing the generalized  $f$ -sum rule,<sup>8</sup> the diamagnetic current is expressed using the Green function similarly to the paramagnetic term:

$$\mathbf{j}_{\text{ind}}(\mathbf{r}') = 2 \sum_o \text{Re} \left[ \langle \Psi_o^{(0)} | \mathbf{J}^p(\mathbf{r}') \mathcal{G}(\epsilon_o) H^{(1)} | \Psi_o^{(0)} \rangle - \langle \Psi_o^{(0)} | \mathbf{J}^p(\mathbf{r}') \mathcal{G}(\epsilon_o) \frac{\mathbf{B} \times \mathbf{r}'}{2c} \cdot \mathbf{v} | \Psi_o^{(0)} \rangle \right], \quad (14)$$

where  $\mathbf{v} = 1/i[\mathbf{r}, H^{(0)}]$ . Combining these two terms together, we arrive at a more compact formula for the induced current:

$$\mathbf{j}_{\text{ind}}(\mathbf{r}') = \frac{1}{c} \sum_o \text{Re} \left[ \langle \Psi_o^{(0)} | \mathbf{J}^p(\mathbf{r}') \mathcal{G}(\epsilon_o) ((\mathbf{r} - \mathbf{r}') \times \mathbf{p} \cdot \mathbf{B}) | \Psi_o^{(0)} \rangle \right]. \quad (15)$$

As mentioned before, in an extended system the position operator is not well defined. This difficulty can be overcome by modulating either the magnetic field<sup>6</sup> or the position operator.<sup>8</sup> We follow the latter choice, where the position operator is replaced with the limit:

$$(\mathbf{r} - \mathbf{r}') \cdot \hat{\mathbf{u}}_i = \lim_{q \rightarrow 0} \frac{1}{2q} [e^{iq\hat{\mathbf{u}}_i \cdot (\mathbf{r} - \mathbf{r}')} - e^{-iq\hat{\mathbf{u}}_i \cdot (\mathbf{r} - \mathbf{r}')}], \quad (16)$$

where  $\hat{\mathbf{u}}$  is the unit vector of the Cartesian frame of reference, and  $q$  is the modulation wave vector. Consequently, the induced current has to be evaluated by taking the limit

$$\mathbf{j}_{\text{ind}}(\mathbf{r}') = \lim_{q \rightarrow 0} \frac{1}{2q} [\mathbf{S}(\mathbf{r}', q) - \mathbf{S}(\mathbf{r}', -q)], \quad (17)$$

where  $\mathbf{S}(\mathbf{r}', \mathbf{q})$  is defined as

$$\mathbf{S}(\mathbf{r}', q) = \frac{1}{c} \sum_{x,y,z} \sum_o \text{Re} \left[ \frac{1}{i} \langle \Psi_o^{(0)} | \mathbf{J}^p(\mathbf{r}') \mathcal{G}(\epsilon_o) \times \mathbf{B} \times \hat{\mathbf{u}}_i \cdot e^{iq\hat{\mathbf{u}}_i \cdot (\mathbf{r} - \mathbf{r}')} \mathbf{p} | \Psi_o^{(0)} \rangle \right]. \quad (18)$$

The sum in this formula runs over all occupied states. For periodic systems, this involves a summation over the whole Brillouin zone. However, in this case, the eigenvectors are Bloch functions  $\Psi_{i,\mathbf{k}}^{(0)}(\mathbf{r}) = e^{i\mathbf{k} \cdot \mathbf{r}} u_{i,\mathbf{k}}^{(0)}$ , and the matrix elements of the paramagnetic current operator are diagonal with respect to the  $k$  vector. Therefore we define a  $\mathbf{k}$ -dependent Green function

$$\mathcal{G}_{\mathbf{k}}(\epsilon) = \sum_e \frac{|u_{e,\mathbf{k}}^{(0)}\rangle \langle u_{e,\mathbf{k}}^{(0)}|}{\epsilon - \epsilon_{e,\mathbf{k}}}, \quad (19)$$

and the paramagnetic current operator in the basis of Bloch states

$$\mathbf{J}_{\mathbf{k},\mathbf{k}'}^p(\mathbf{r}') = - \frac{(-i\nabla + \mathbf{k})|\mathbf{r}'\rangle \langle \mathbf{r}'| + |\mathbf{r}'\rangle \langle \mathbf{r}'| (-i\nabla + \mathbf{k}')}{2}, \quad (20)$$

the expression for  $\mathbf{S}(\mathbf{r}', \mathbf{q})$  in the periodic system can be written as

$$\mathbf{S}(\mathbf{r}', q) = \frac{1}{cN_{\mathbf{k}}} \sum_{\alpha=x,y,z} \sum_{o,\mathbf{k}} \text{Re} \left[ \frac{1}{i} \langle u_{o,\mathbf{k}}^{(0)} | \mathbf{J}_{\mathbf{k},\mathbf{k}+\mathbf{q}_\alpha}^p(\mathbf{r}') \times \mathcal{G}_{\mathbf{k}+\mathbf{q}_\alpha}(\epsilon_o) \mathbf{B} \times \hat{\mathbf{u}}_i \cdot \mathbf{v}_{\mathbf{k},\mathbf{k}+\mathbf{q}_\alpha} | u_{o,\mathbf{k}}^{(0)} \rangle \right], \quad (21)$$

where  $\mathbf{v}_{\mathbf{k},\mathbf{k}'} = -i\nabla + \mathbf{k}'$ . Equation (17) together with Eq. (21) constitute the final expressions for computing the current density, which is valid for any full-potential method. A more detailed derivation of these formulas can be found in Refs. 8 and 21 for the PAW and ultrasoft pseudopotential framework. In the following section, we apply it to the particular case of the LAPW basis set.

## B. Induced current in LAPW

In the LAPW method,<sup>35</sup> the unit cell is partitioned into nonoverlapping atomic spheres ( $S_\alpha$ ) centered on the nuclei, and the interstitial region. The basis functions are plane waves in the interstitial region, that are augmented by a linear combination of spherical harmonics times corresponding radial functions inside each atomic sphere:

$$\phi_{\mathbf{k},\mathbf{G}}^{\text{LAPW}}(\mathbf{r}) = \begin{cases} \frac{1}{\sqrt{\Omega}} e^{i(\mathbf{G}+\mathbf{k}) \cdot \mathbf{r}}, & \mathbf{r} \in I, \\ \sum_{lm} [A_{lm}^{\alpha,\mathbf{k}+\mathbf{G}} u_l^\alpha(r, E_l) + B_{lm}^{\alpha,\mathbf{k}+\mathbf{G}} \dot{u}_l^\alpha(r, E_l)] Y_{lm}(\hat{r}), & \mathbf{r} \in S_\alpha, \end{cases} \quad (22)$$

where  $A_{lm}^{\alpha,\mathbf{k}+\mathbf{G}}$  and  $B_{lm}^{\alpha,\mathbf{k}+\mathbf{G}}$  are derived such that the basis functions are continuous in value and slope at the sphere boundary of each atom. The radial functions  $u_l(r, E_l)$  are the solutions of the scalar relativistic Schrödinger equation in a spherical potential evaluated at the energies  $E_l$ , where  $l$  denotes the angular momentum quantum number.  $\dot{u}_l$  is the energy derivative of  $u_l(r, E_l)$  taken at  $E_l$ . The LAPW basis functions capture efficiently the energy dependence of the radial wave function around the energies  $E_l$  due to the presence of the  $\dot{u}_l$  term. However, in order to cover a larger energy region, for instance, at energies where the number of nodes of the radial function is different from that at  $E_l$  (semicore states or higher conduction band states), additional radial basis functions are supplied in form of so-called local orbitals (LO):

$$\phi_{lm,\mathbf{k}}^{\text{LO},\alpha,i}(\mathbf{r}) = \begin{cases} 0, & \mathbf{r} \in I, \\ \left[ A_{lm}^{i,\alpha,\mathbf{k}} u_l^\alpha(r, E_l) + B_{lm}^{i,\alpha,\mathbf{k}} \dot{u}_l^\alpha(r, E_l) + C_{lm}^{i,\alpha,\mathbf{k}} u_l^{\alpha,i}(r, E_l^i) \right] Y_{lm}(\hat{r}), & \mathbf{r} \in S_\alpha. \end{cases} \quad (23)$$

The local orbitals vanish at the sphere boundary and in the interstitial, therefore they are not coupled to the plane waves. The  $A_{lm}^{\alpha,\mathbf{k}}$ ,  $B_{lm}^{\alpha,\mathbf{k}}$ , and  $C_{lm}^{\alpha,\mathbf{k}}$  are determined from normalization and ‘‘continuity in value and slope’’ conditions. In the APW + lo<sup>37,38</sup> formulation for the linearization, the continuous slope condition has been dropped and the linearization term containing  $\dot{u}_l(r, E_l)$  is moved to an additional local orbital (lo). Consequently, for both the LAPW and APW + lo method, the resulting wave functions are represented as a Fourier series in the interstitial region and as a ( $lm$ ) series inside the spheres:

$$\Psi_{n,\mathbf{k}}(\mathbf{r}) = \begin{cases} \frac{1}{\sqrt{\Omega}} \sum_{\mathbf{G}} C_{\mathbf{G}}^n e^{i(\mathbf{G}+\mathbf{k}) \cdot \mathbf{r}}, & \mathbf{r} \in I, \\ \sum_{lm} W_{lm}^{n,\alpha,\mathbf{k}}(r) Y_{lm}(\hat{r}), & \mathbf{r} \in S_\alpha, \end{cases} \quad (24)$$

where the expression for  $W_{lm}^{n,\alpha,\mathbf{k}}(r)$  involves summation over the reciprocal lattice vectors  $\mathbf{G}$  and different radial functions used to define augmented plane waves and local orbitals:

$$W_{lm}^{n,\alpha,\mathbf{k}}(r) = \sum_{\mathbf{G},i} C_{\mathbf{G},i} [A_{lm}^{\alpha,\mathbf{k},\mathbf{G},i} u_l^\alpha(r, E_l) + B_{lm}^{\alpha,\mathbf{k},\mathbf{G},i} u_l^\alpha(r, E_l) + C_{lm}^{i,\alpha,\mathbf{k}} u_l^{\alpha,i}(r, E_l^i)] Y_{lm}(\hat{r}). \quad (25)$$

Such an expansion of the wave function allows to describe its true nodal structure without any approximations. This is true also for any quantity that is computed from the wave functions (e.g., the charge density). Following an APW style, we represent our induced current density as a Fourier series in the interstitial and a spherical harmonics expansion inside the spheres:

$$\mathbf{j}_{\text{ind}}(\mathbf{r}) = \begin{cases} \sum_{\mathbf{G}} \text{Re}[\mathbf{j}_{\mathbf{G}} e^{i\mathbf{G}\cdot\mathbf{r}}], & \mathbf{r} \in I, \\ \sum_{lm} \text{Re}[\mathbf{j}_{lm}^\alpha(r) Y_{lm}(\hat{r})], & \mathbf{r} \in S_\alpha, \end{cases} \quad (26)$$

where  $\mathbf{j}_{\mathbf{G}}$  are the Fourier coefficients and  $\mathbf{j}_{lm}^\alpha(r)$  are radial functions that depend only on the distance from the nucleus  $\alpha$ . Following Eq. (17), both  $\mathbf{j}_{\mathbf{G}}$  and  $\mathbf{j}_{lm}^\alpha(r)$  are expressed as finite derivatives:

$$\mathbf{j}_{\mathbf{G}} = \lim_{q \rightarrow 0} \frac{1}{2q} [\mathbf{S}_{\mathbf{G}}(q) - \mathbf{S}_{\mathbf{G}}(-q)], \quad (27)$$

$$\mathbf{j}_{lm}^\alpha(r) = \lim_{q \rightarrow 0} \frac{1}{2q} [\mathbf{S}_{lm}(r, q) - \mathbf{S}_{lm}(r, -q)]. \quad (28)$$

This becomes obvious when we write  $S(\mathbf{r}, q)$  from Eq. (21) in the following form:

$$\mathbf{S}(\mathbf{r}, q) = \frac{1}{cN_{\mathbf{k}}} \sum_{\alpha=x,y,z} \sum_{\mathbf{k}} \sum_o \left\{ \frac{1}{i} [\mathbf{A}_{\mathbf{k},q_\alpha}^o(\mathbf{r}) + \mathbf{B}_{\mathbf{k},q_\alpha}^o(\mathbf{r})] \right\}, \quad (29)$$

where  $\mathbf{A}_{\mathbf{k},q_\alpha}^o(\mathbf{r})$  and  $\mathbf{B}_{\mathbf{k},q_\alpha}^o(\mathbf{r})$  are

$$\mathbf{A}_{\mathbf{k},q_\alpha}^o(\mathbf{r}') = \langle u_{o,\mathbf{k}} | (\mathbf{p} + \mathbf{k}) | \mathbf{r}' \rangle \langle \mathbf{r}' | u_{o,\mathbf{k}+\mathbf{q}_\alpha}^{(1)} \rangle, \quad (30)$$

$$\mathbf{B}_{\mathbf{k},q_\alpha}^o(\mathbf{r}') = \langle u_{o,\mathbf{k}} | \mathbf{r}' \rangle \langle \mathbf{r}' | (\mathbf{p} + \mathbf{k} + \mathbf{q}_\alpha) | u_{o,\mathbf{k}+\mathbf{q}_\alpha}^{(1)} \rangle, \quad (31)$$

and the periodic part of the perturbed wave function  $|u_{o,\mathbf{k}+\mathbf{q}_\alpha}^{(1)}\rangle$  is evaluated with

$$|u_{o,\mathbf{k}+\mathbf{q}_\alpha}^{(1)}\rangle = (\mathbf{B} \times \hat{\alpha}) \cdot G_{\mathbf{k}+\mathbf{q}_\alpha}(\epsilon_o) |(\mathbf{p} + \mathbf{k}) | u_{o,\mathbf{k}} \rangle. \quad (32)$$

The quantities  $\mathbf{A}_{\mathbf{k},q_\alpha}^o(\mathbf{r}')$  and  $\mathbf{B}_{\mathbf{k},q_\alpha}^o(\mathbf{r}')$  are the vector fields represented using plane waves and spherical harmonics in the interstitial and inside spheres, respectively. The Fourier components  $\mathbf{S}_{\mathbf{G}}(\mathbf{q})$  are computed by multiplying the corresponding components ( $\langle u_{o,\mathbf{k}} | \mathbf{p} | \mathbf{r}' \rangle$  and  $\langle u_{o,\mathbf{k}} | \mathbf{r}' \rangle$ ) and the step function on a real-space mesh, and after that transforming the result to reciprocal space. Due to the specific representation of the wave function inside the atomic spheres, its periodic part is not easily accessible. Therefore, in order to calculate the induced current inside the spheres, it is more efficient to rewrite Eqs. (30)–(31) using the full Bloch wave function:

$$\mathbf{A}_{\mathbf{k},q_\alpha}^{o,e}(\mathbf{r}') = e^{-i\mathbf{q}\cdot\mathbf{r}'} \langle \Psi_{o,\mathbf{k}} | \mathbf{p} | \mathbf{r}' \rangle \langle \mathbf{r}' | \Psi_{o,\mathbf{k}+\mathbf{q}_\alpha}^{(1)} \rangle, \quad (33)$$

$$\mathbf{B}_{\mathbf{k},q_\alpha}^{o,e}(\mathbf{r}') = e^{-i\mathbf{q}\cdot\mathbf{r}'} \langle \Psi_{o,\mathbf{k}} | \mathbf{r}' \rangle \langle \mathbf{r}' | \mathbf{p} | \Psi_{o,\mathbf{k}+\mathbf{q}_\alpha}^{(1)} \rangle, \quad (34)$$

where the perturbation  $|\Psi_{o,\mathbf{k}+\mathbf{q}_\alpha}^{(1)}\rangle$  is given by

$$|\Psi_{o,\mathbf{k}+\mathbf{q}_\alpha}^{(1)}\rangle = (\mathbf{B} \times \hat{\alpha}) \cdot G_{\mathbf{k}+\mathbf{q}_\alpha}(\epsilon_o) |e^{i\mathbf{q}\cdot\mathbf{r}} \mathbf{p} | \Psi_{o,\mathbf{k}} \rangle. \quad (35)$$

$|u_{o,\mathbf{k}+\mathbf{q}_\alpha}^{(1)}\rangle$  defined in Eq. (32) is the periodic part of  $|\Psi_{o,\mathbf{k}+\mathbf{q}_\alpha}^{(1)}\rangle$ . Applying Eq. (32) or (35) requires the evaluation of matrix elements between occupied and all empty states,

$$C_{\mathbf{k},q_\alpha}^{o,e} = (\mathbf{B} \times \hat{\alpha}) \cdot \langle \Psi_{e,\mathbf{k}+\mathbf{q}_\alpha} | e^{i\mathbf{q}\cdot\mathbf{r}} \mathbf{p} | \Psi_{o,\mathbf{k}} \rangle. \quad (36)$$

Alternatively, the  $|\Psi_{o,\mathbf{k}+\mathbf{q}_\alpha}^{(1)}\rangle$  can be calculated by solving the linear equation

$$(\epsilon_o - H^{(0)}) |\Psi_{o,\mathbf{k}+\mathbf{q}_\alpha}^{(1)}\rangle = Q H^{(1)} |\Psi_{o,\mathbf{k}}\rangle, \quad (37)$$

where  $Q = 1 - \sum_o |\Psi_{o,\mathbf{k}+\mathbf{q}}\rangle \langle \Psi_{o,\mathbf{k}+\mathbf{q}}|$  is the projector operator on the empty states,  $H^{(0)}$  is the unperturbed Hamiltonian, and  $H^{(1)}$  is the perturbation equal to  $(\mathbf{B} \times \hat{\alpha}) e^{i\mathbf{q}\cdot\mathbf{r}} \mathbf{p}$ . In this case, only matrix elements between occupied states at  $\mathbf{k}$ -points  $\mathbf{k}$  and  $\mathbf{k} + \mathbf{q}$  need to be addressed. In the case of plane-wave based methods, the alternative root has certainly the computational advantage, however, in LAPW, the size of Hamiltonian is rather moderate and the first option is no longer arduous and in solids it seems to be computationally more efficient.

Because the modulation vector  $q$  is small, the function  $e^{i\mathbf{q}\cdot\mathbf{r}}$  inside each sphere can be approximated by

$$e^{i\mathbf{q}\cdot\mathbf{r}'} = e^{i\mathbf{q}\cdot\mathbf{r}_\alpha} e^{i\mathbf{q}\cdot(\mathbf{r}'-\mathbf{r}_\alpha)} \approx e^{i\mathbf{q}\cdot\mathbf{r}_\alpha} [1 + i\mathbf{q} \cdot (\mathbf{r}' - \mathbf{r}_\alpha)], \quad (38)$$

where  $r_\alpha$  is the position of an atom,  $\mathbf{r} = \mathbf{r}' - \mathbf{r}_\alpha$ ,  $r = |\mathbf{r}' - \mathbf{r}_\alpha|$ . Further, the vector  $(\mathbf{r} - \mathbf{r}_\alpha)$  is conveniently expressed using spherical harmonics  $Y_{1,m}(\hat{\mathbf{r}})$ :

$$(\mathbf{r} - \mathbf{r}_\alpha)_x = -\sqrt{\frac{2\pi}{3}} r [Y_{1,1}(\hat{\mathbf{r}}) - Y_{1,-1}(\hat{\mathbf{r}})], \quad (39)$$

$$(\mathbf{r} - \mathbf{r}_\alpha)_y = i\sqrt{\frac{2\pi}{3}} r [Y_{1,1}(\hat{\mathbf{r}}) + Y_{1,-1}(\hat{\mathbf{r}})], \quad (40)$$

$$(\mathbf{r} - \mathbf{r}_\alpha)_z = \sqrt{\frac{4\pi}{3}} r Y_{1,0}(\hat{\mathbf{r}}), \quad (41)$$

where  $(\mathbf{r} - \mathbf{r}_\alpha)_{x,y,z}$  are the Cartesian coordinates of  $(\mathbf{r} - \mathbf{r}_\alpha)$ . Introducing Eqs. (38) and (24) into Eqs. (33)–(36) and taking derivatives according to Eq. (A1), we derive expressions involving products of three spherical harmonics. Such products can be further expanded into a series of spherical harmonics:

$$Y_{l'm'} Y_{lm}^* Y_{l''m''} = \sum_{LM} \left[ \sum_{L'M'} G_{L'L'L''}^{m'M'm''} G_{LL'L}^{mM'M} \right] Y_{LM},$$

where  $G_{LL'L}^{mM'M} = \int Y_{lm} Y_{l'm'} Y_{Lm}^*$  are the Gaunt coefficient. This allows to determine the radial expansion coefficients of  $\mathbf{A}_{\mathbf{k},q_\alpha}^o(\mathbf{r}')$  and  $\mathbf{B}_{\mathbf{k},q_\alpha}^o(\mathbf{r}')$  for each  $LM$ . The final formulas are presented in Appendix B.

### C. Integration of the current density

In the next step, we integrate the current density  $j_{\text{ind}}(\mathbf{r})$  according to Eq. (2). For this, we apply a method that is a modification of the pseudocharge approach developed by Weinert.<sup>39</sup> Weinert's method has been originally developed and used for solving Poisson's equation in the full-potential LAPW method. The main reason for using this approach is, of

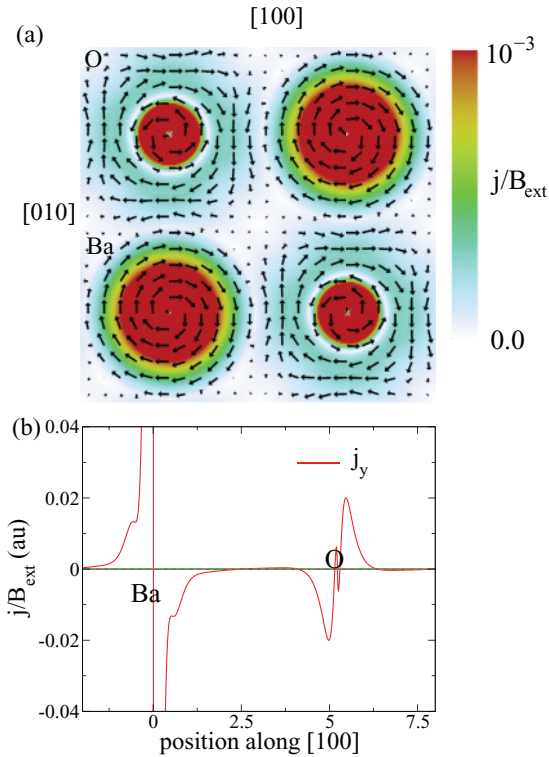


FIG. 1. (Color online) The induced current density  $\mathbf{j}_{\text{ind}}(\mathbf{r})$  calculated for an external field applied in the [001] direction. The density is plotted in a plane perpendicular to the external field cutting through Ba and O atoms. The color map in (a) represents the magnitude of the current density, while the arrows give the direction of the current vector, and (b) shows the (010) component of  $\mathbf{j}_{\text{ind}}(\mathbf{r})$  along [100] direction.

course, the fact that for infinite periodic systems, the integral in Eq. (2) does not necessarily converge, and the effects related to the size and shape of the sample have to be included. Those finite-size effects are easily managed by transforming the integral into reciprocal space. However, such a transformation is not feasible due to the localized and oscillatory nature of the all-electron current density (see, for instance, Fig. 1).

Before we present our procedure in detail, we will first have a closer look at the particular contributions to the Biot-Savart integral. As we can see in Fig. 1, the current density is relatively low in the interstitial region and large around the nuclei. Therefore we may expect that the contributions to the induced field originating from the interstitial region and the neighboring spheres are small. Indeed, as shown in Fig. 2, the value of the integrand in Eq. (2) is small in the interstitial and oscillates around zero inside neighboring spheres. Furthermore, the main contribution to the absolute shift comes from a relatively small volume around the nuclei, as indicated in Fig. 2(c). Table I compares the contributions to the isotropic shift from the atomic sphere to the total shift calculated over all space. As we see, most of the shift for a given nucleus is generated by the current inside the atom. This statement is, in particular, valid for heavier nuclei and for ionic compounds, but lighter nuclei and/or compounds with strong covalent bonds have larger contributions from outside the sphere. Although the difference is sometimes only a few

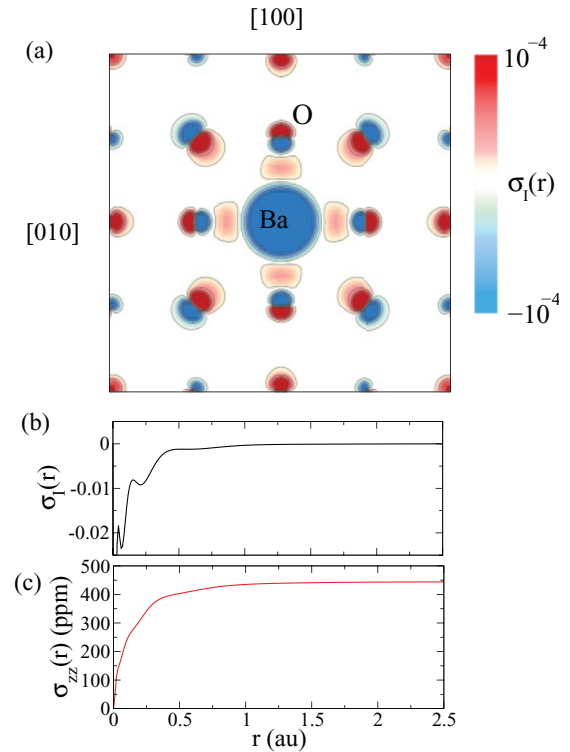


FIG. 2. (Color online) (a)  $\sigma_I(\mathbf{r}) = [\mathbf{j}_{\text{ind}}(\mathbf{r}) \times \frac{\mathbf{R}-\mathbf{r}}{|\mathbf{R}-\mathbf{r}|^3}]_z$  [the [001] component of the integrand of Eq. (2)] calculated for BaO.  $\mathbf{R}$  points to the central Ba atom, the external field points in the [001] direction, the plotting plane is perpendicular to [001] and cuts through Ba and O atoms. (b)  $4\pi r^2 \sigma_I(\mathbf{r})$  plotted inside the central Ba sphere. (c) Partial shielding  $\sigma_{zz}(r') = -\int_0^{r'} dr' [4\pi r'^2 \mathbf{j}_{\text{ind}}(\mathbf{r}') \times \frac{\mathbf{R}-\mathbf{r}'}{|\mathbf{R}-\mathbf{r}'|^3}]_z$  as a function of the integration radius  $r$  plotted inside the Ba sphere.

ppm, it is far above the accuracy we would like to reach when computing NMR shifts. Therefore an integration that goes beyond the atomic sphere is necessary.

Our approach is based on the fact that the contribution to the magnetic field induced at the nucleus at  $\mathbf{R}_1$  originating from a current inside a sphere centered at a different nucleus at  $\mathbf{R}_2$

TABLE I. Comparison of the total isotropic shielding  $\sigma_{\text{tot}}$  with the integral over the atomic sphere only ( $\sigma_{\text{sph}}$ ) in ppm.

	$\sigma_{\text{tot}}$	$\sigma_{\text{sph}}$	$\sigma_{\text{tot}} - \sigma_{\text{sph}}$
BaO (O)	-455.6	-464.9	9.3
BaO (Ba)	4519.8	4521.6	-1.8
MgO (O)	204.5	197.7	6.8
MgO (Mg)	5709.0	5742.3	-33.3
SrF <sub>2</sub> (F)	226.0	232.1	-6.1
SrF <sub>2</sub> (Sr)	2996.2	3002.8	-6.6
NaF (F)	406.3	404.4	-1.9
NaF (Na)	572.8	578.5	-5.7
Si	413.6	399.6	14
diamond	141.3	117.7	23.6
CF <sub>4</sub> (F)	232	205	27
CF <sub>4</sub> (C)	38	17	11
CH <sub>4</sub> (H)	31	9	22
CH <sub>4</sub> (C)	194	163	30

depends solely on the multipole moments of the current in this sphere, but not on the detailed shape of the current. Therefore it is possible to replace the current density inside neighboring spheres with another more convenient pseudodensity, which has identical multipole moments. The algorithm we use to calculate the induced field can be summarized as follows. According to Eq. (26), the Fourier expansion is valid only in the interstitial region. Inside the spheres, we use a spherical harmonics expansion. Because a Fourier expansion is easy to integrate over the whole unit cell, we let the plane waves enter the spheres and correct the corresponding spherical harmonics expansion inside the spheres. This can be done by expanding the plane waves inside the spheres into spherical harmonics and spherical Bessel functions  $j_l(Gr)$ :

$$e^{i\mathbf{G}\mathbf{r}} = \sum_{lm} 4\pi i^l j_l(Gr) Y_{lm}^*(\hat{\mathbf{G}}) Y_{lm}(\hat{\mathbf{r}}), \quad (42)$$

and the corrected current expansion is

$$\mathbf{j}_{\text{ind}}(\mathbf{r}) = \begin{cases} \sum_{\mathbf{G}} \mathbf{j}_{\mathbf{G}} e^{i\mathbf{G}\cdot\mathbf{r}}, & \mathbf{r} \in \Omega, \\ \sum_{lm} \mathbf{j}_{lm}^{\alpha,c}(r) Y_{lm}(\hat{\mathbf{r}}), & \mathbf{r} \in S_{\alpha}, \end{cases} \quad (43)$$

where  $\mathbf{j}_{lm}^{\alpha,c}(r) = \mathbf{j}_{lm}^{\alpha}(r) - 4\pi \sum_{\mathbf{G}} \mathbf{j}_{\mathbf{G}} i^l j_l(Gr) Y_{lm}^*(\hat{\mathbf{G}})$ . Next, we determine for each sphere a pseudocurrent density:

$$\tilde{\mathbf{j}}_{\alpha}(\mathbf{r}) = \sum_{lm} \mathbf{Q}_{lm}^{\alpha} Y_{lm}(\hat{\mathbf{r}}) \sum_{\eta} a_{\eta} r^{\nu_{\eta}}, \quad \mathbf{r} \in S_{\alpha}, \quad (44)$$

where  $\mathbf{Q}_{lm}^{\alpha}$ ,  $\mathbf{a}_{\eta}$ , and  $\nu_{\eta}$  are chosen such that the multipole moments of the pseudo-current-density are equal to the multipole moments  $\tilde{\mathbf{q}}_{lm}^{\alpha}$  of the  $\mathbf{j}_{lm}^{\alpha,c}(r)$  component of the current in Eq. (43). This can be written in a compact form as

$$\begin{aligned} \tilde{\mathbf{q}}_{lm}^{\alpha} &= \mathbf{q}_{lm}^{\alpha} - \mathbf{q}_{lm}^{PW_{\alpha}}, \\ \mathbf{q}_{lm}^{\alpha} &= \int_{S_{\alpha}} d^3r Y_{lm}^*(\hat{\mathbf{r}}) r^l \mathbf{j}_{\text{ind}}(\mathbf{r}), \\ \mathbf{q}_{lm}^{PW_{\alpha}} &= \frac{\sqrt{4\pi}}{3} R_{\alpha}^3 \mathbf{j}_{\mathbf{G}=0} \delta_{l0} \\ &+ \sum_{\mathbf{G} \neq 0} 4\pi \mathbf{j}_{\mathbf{G}} R_{\alpha}^{l+3} \frac{j_{l+1}(GR_{\alpha})}{GR_{\alpha}} e^{i\mathbf{G}\xi_{\alpha}} Y_{lm}^*(\mathbf{G}), \end{aligned} \quad (45)$$

where  $\mathbf{q}_{lm}^{\alpha}$  are the multiple moments of the current inside spheres and  $\mathbf{q}_{lm}^{PW_{\alpha}}$  are the moments of the plane waves entering the spheres. The parameters  $\mathbf{Q}_{lm}^{\alpha}$  are proportional to  $\tilde{\mathbf{q}}_{lm}^{\alpha}$ ,

$$\mathbf{Q}_{lm}^{\alpha} = \tilde{\mathbf{q}}_{lm}^{\alpha} \left[ \sum_{\eta} a_{\eta} \frac{R_{\alpha}^{l+\nu_{\eta}+3}}{l+\nu_{\eta}+3} \right]^{-1}. \quad (46)$$

In the interstitial region, the pseudocurrent is by definition zero, and we calculate the Fourier transform of the pseudocurrent:

$$\tilde{\mathbf{j}}_{\mathbf{G}} = \frac{1}{\Omega} \int d^3\mathbf{r} \left[ \sum_{\alpha} \tilde{\mathbf{j}}_{\alpha}(\mathbf{r}) \right] e^{-i\mathbf{G}\mathbf{r}}, \quad (47)$$

$\tilde{\mathbf{j}}_{\mathbf{G}}$  can be evaluated with the following expression:

$$\begin{aligned} \tilde{\mathbf{j}}_{\mathbf{G}} &= \frac{4\pi}{\Omega} \sum_{lm,\alpha} \frac{(-i)^l (2l+2n+3)!!}{(2l+1)!!} \\ &\times \frac{j_{l+n+1}(GR_{\alpha})}{(GR_{\alpha})^{n+1}} \mathbf{q}_{lm}^{\alpha} e^{-i\mathbf{G}\xi_{\alpha}} Y_{lm}(\hat{\mathbf{G}}). \end{aligned} \quad (48)$$

In the next step, the pseudocurrent is added to the plane-wave component of the current density and accordingly subtracted from the spherical harmonic part inside spheres:

$$\mathbf{j}_{\text{ind}}(\mathbf{r}) = \begin{cases} \sum_{\mathbf{G}} (\mathbf{j}_{\mathbf{G}} + \tilde{\mathbf{j}}_{\mathbf{G}}) e^{i\mathbf{G}\cdot\mathbf{r}}, & \mathbf{r} \in \Omega, \\ \sum_{lm} [\mathbf{j}_{lm}^{\alpha,c}(r) - \tilde{\mathbf{j}}_{\alpha}(\mathbf{r})] Y_{lm}(\hat{\mathbf{r}}), & \mathbf{r} \in S_{\alpha}. \end{cases} \quad (49)$$

At this point, the multipole moments of the current inside spheres are equal to zero. This means that all spheres except the one centered at the nucleus at which the induced field is calculated (central sphere) do not contribute to the Biot-Savart integral [see Eq. (2)]. The component of the current density represented with the Fourier series correctly accounts for all contributions except from the central sphere. The contribution from this sphere can be calculated by integrating  $\mathbf{j}_{\text{ind}}^{S,\alpha}(\mathbf{r}) = \sum_{lm} [\mathbf{j}_{lm}^{\alpha,c}(r) - \tilde{\mathbf{j}}_{\alpha}(\mathbf{r})] Y_{lm}(\hat{\mathbf{r}})$ . For the sphere at  $\mathbf{R} = 0$ , Eq. (2) simplifies to

$$\mathbf{B}_{\text{ind}}^{S,\alpha}(0) = -\frac{1}{c} \int_{\alpha} d^3r \mathbf{j}_{\text{ind}}(\mathbf{r}) \times \frac{\hat{\mathbf{r}}}{|\mathbf{r}|^2}. \quad (50)$$

Gathering Eqs. (39)–(41) and (43) into this equation, we arrive at the following expression for the sphere contribution to the induced magnetic field:

$$\begin{aligned} \mathbf{B}_{\text{ind}}^{S,\alpha}(0) &= \frac{1}{c} \sqrt{\frac{4\pi}{3}} \sum_{lm} \left[ \int_0^R dr \mathbf{j}_{\text{ind}}^q(\mathbf{r}) \right] \left[ \frac{1}{\sqrt{2}} (G_{l01}^{m01} - G_{l01}^{m0-1}), \right. \\ &\quad \left. \frac{i}{\sqrt{2}} (G_{l01}^{m01} + G_{l01}^{m0-1}), G_{l01}^{m00} \right]. \end{aligned} \quad (51)$$

The plane-wave component of the induced current is easily integrated in reciprocal space. The Fourier transformation of the Eq. (2) leads to

$$\mathbf{B}_{\text{ind}}^{\text{PW}}(\mathbf{G}) = \frac{4\pi}{c} \frac{i\mathbf{G} \times (\mathbf{j}_{\mathbf{G}} + \tilde{\mathbf{j}}_{\mathbf{G}})}{G^2}, \quad (52)$$

which is valid only for  $\mathbf{G} \neq 0$ . The  $\mathbf{G} = 0$  term corresponds to the uniform field and it is determined by the shape of the sample and the macroscopic magnetic susceptibility  $\overleftrightarrow{\chi}$  tensor. Adopting the experimental convention, we assume a spherical sample for which

$$\mathbf{B}_{\text{ind}}^{\text{PW}}(\mathbf{G} = 0) = \frac{8\pi}{3} \overleftrightarrow{\chi} \mathbf{B}. \quad (53)$$

The value of the induced field at the nucleus can be calculated by back transformation

$$\mathbf{B}_{\text{ind}}^{\text{PW},\alpha}(\mathbf{R}_{\alpha}) = \sum_{\mathbf{G}} \mathbf{B}_{\text{ind}}(\mathbf{G}) e^{i\mathbf{G}\mathbf{R}_{\alpha}}. \quad (54)$$

Finally, the total induced magnetic field evaluated at the nucleus  $\alpha$  is equal to

$$\mathbf{B}_{\text{ind}}^{\alpha}(\mathbf{R}_{\alpha}) = \mathbf{B}_{\text{ind}}^{\text{PW},\alpha}(\mathbf{R}_{\alpha}) + \mathbf{B}_{\text{ind}}^{S,\alpha}(\mathbf{R}_{\alpha}). \quad (55)$$

In order to calculate the macroscopic susceptibility  $\overleftrightarrow{\chi}$ , which enters  $\mathbf{B}_{\text{ind}}^{\text{PW}}(\mathbf{G} = 0)$ , we follow Mauri and Pickard<sup>8</sup> and use

$$\overleftrightarrow{\chi} = \lim_{q \rightarrow 0} \frac{\overleftrightarrow{F}(q) - 2\overleftrightarrow{F}(0) + \overleftrightarrow{F}(-q)}{q^2}, \quad (56)$$

where  $F_{i,j} = (2 - \delta_{i,j})Q_{i,j}$  and  $i$  and  $j$  are the indices of the Cartesian coordinates. The tensor  $\overleftrightarrow{Q}$  is calculated with

$$\overleftrightarrow{Q}(q) = \frac{1}{N_k \Omega c^2} \sum_{\alpha=x,y,z} \sum_{o,k} \text{Re}[\mathbf{A}_{\mathbf{k},\mathbf{q}_\alpha}^o (\mathbf{A}_{\mathbf{k},\mathbf{q}_\alpha}^o)^*], \quad (57)$$

where  $\mathbf{A}_{\mathbf{k},\mathbf{q}_\alpha}^o$  are the matrix elements between Bloch states at  $\mathbf{k}$  and  $\mathbf{k} + \mathbf{q}_\alpha$ :

$$\mathbf{A}_{\mathbf{k},\mathbf{q}_\alpha}^o = \hat{\alpha} \times \langle u_{o,\mathbf{k}} | (\mathbf{p} + \mathbf{k}) | u_{\mathbf{k}+\mathbf{q}_\alpha}^{(1)} \rangle. \quad (58)$$

The  $\langle u_{o,\mathbf{k}} | (\mathbf{p} + \mathbf{k}) | u_{\mathbf{k}+\mathbf{q}_\alpha}^{(1)} \rangle$  are the components of the factors  $C_{\mathbf{k},\mathbf{q}}^o$  that appear in the expression for the current density and are defined in Eq. (B10).

#### D. Core component

In our implementation of the LAPW method, the core states are calculated by solving the Dirac equation with the spherical part of the self-consistent potential. The core-valence separation is determined with respect to the amount of core charge that leaks out of the atomic sphere. In practice, we require that each core orbital has more than 99.5% of its charge inside the sphere, which usually results in a core-valence energy threshold around 5–7 Ry below the top of the valence bands. This also insures good orthogonality between core and valence states. In the symmetric gauge centered at the nucleus, the paramagnetic component of the induced current is zero, and only the diamagnetic contribution needs to be considered:

$$\mathbf{j}_{\text{ind}}(\mathbf{r}') = -\frac{1}{2c} \rho_{\text{core}}(\mathbf{r}') \mathbf{B} \times \mathbf{r}'. \quad (59)$$

Expressing  $\mathbf{r}'$  as combination of  $Y_{lm}$  spherical harmonics as in Eqs. (39)–(41) and assuming that the core density  $\rho_{\text{core}}(\mathbf{r}')$  is spherical, the  $LM$  component of the core contribution to the induced current is

$$\begin{aligned} \mathbf{j}_{\text{ind}}^{LM}(r) = & -\frac{1}{c} \sqrt{\frac{\pi}{6}} r \rho_{\text{core}}(r) \mathbf{B} \\ & \times [G_{1L0}^{-1M0} - G_{1L0}^{1M0}, i(G_{1L0}^{1M0} + G_{1L0}^{-1M0}), \sqrt{2}G_{1L0}^{0M0}]. \end{aligned} \quad (60)$$

This contribution is added to the current generated by the valence electrons. Afterwards, the total current is integrated using the procedure described in the previous section.

Similarly, the core component of the macroscopic susceptibility is calculated using a formula valid for an isolated atom:

$$\chi_{\text{core}} = -\frac{1}{6\Omega c^2} \sum_{i \in \text{core}} \langle \Psi_i | r^2 | \Psi_i \rangle. \quad (61)$$

### III. NUMERICAL TESTS

#### A. Basis enhancement

The flexibility of the LAPW basis set inside the atomic spheres is limited to the energy region around the linearization energies. Because in the perturbation method, the first-order perturbation of the occupied eigenstates is expressed using the unoccupied orbitals (via Green functions), the standard set of the linearization energies and radial functions, optimal for valence calculations, may not provide enough flexibility for

NMR calculations. A natural way in the LAPW method to extend the flexibility of the basis set is adding additional local orbitals. The concept of LOs has been originally developed for dealing with semicore states,<sup>35</sup> and in such cases the extra radial function is evaluated at an energy close to the semicore eigenvalues. For the NMR calculations, these local orbitals have to be added at high energies. However, there are no clear rules for determining the appropriate linearization energies. As a first approach, the energies have been determined such that the linearization errors of high-energy states are small, i.e., the radial function of a certain  $l$  character at a given eigenstate should be close to the solution of the radial Schrödinger equation in the self-consistent potential at the corresponding eigenvalue. However, it turns out that we do not need to be that strict with the unoccupied states and this rather cumbersome procedure is not necessary. The local orbitals can be added in an almost arbitrary way, for instance, by increasing the linearization energies in regular intervals. The only issue that has to be taken care of is to prevent linear dependency, i.e., to avoid a situation, when two different radial functions are too similar. In order to automatize the procedure and optimize the number of LO's necessary to reach the convergence, we determine them according to the number of nodes of the corresponding radial functions. Consequently, the linearization energies are set such that each of these radial functions has zero value at the sphere boundary, and the number of nodes inside the sphere of subsequent LO's increases by one. This procedure is illustrated in Fig. 3, where we have plotted the first few  $l = 1$  radial functions for the Be atom. The first-order perturbation involves the momentum operator and thus the main character of the perturbed wave function is shifted toward higher orbital quantum number (the momentum operator acting on spherical harmonics  $Y_{lm}$  creates harmonics  $Y_{l+1,m'}$ ). Therefore the enhancement of the basis set is done for orbital quantum numbers up to  $l_{\text{max}} + 1$ , where  $l_{\text{max}}$  is the character of the valence state. These additional LOs will be referred further on as NMR-LO functions.

For a spherical density  $\rho(\mathbf{r})$ , the NMR absolute shift is proportional to the integral

$$\sigma(\mathbf{R}) = \frac{1}{2c^2} \int dr^3 \frac{\rho(\mathbf{r})}{|\mathbf{R} - \mathbf{r}|}, \quad (62)$$

which can be easily evaluated. This creates an opportunity to test our implementation. For that, we have calculated the NMR absolute shifts for several closed shell atoms and

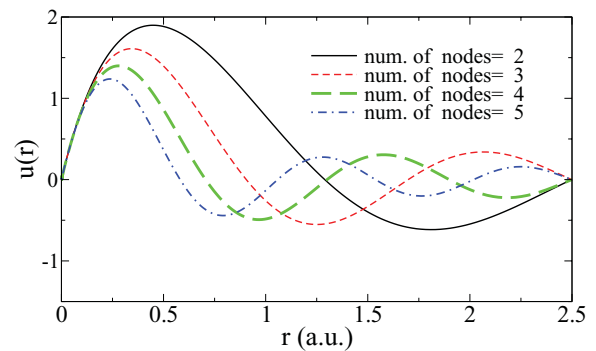


FIG. 3. (Color online) The radial functions associated with the first four NMR LOs of the Be atom with  $p$  character.

compared them with the shifts determined using this simple formula. The atomic reference densities have been obtained by solving the radial Dirac equation within LDA, while the LAPW calculations are performed using a scalar-relativistic Hamiltonian. The results calculated for He, Ar, and Xe are presented in Fig. 4. In all cases, NMR LOs of  $s$ ,  $p$ , and  $d$  character have been added to the basis set. The convergence rate with respect to the number of additional LOs depends on the atom. The calculations for He converge already with five LOs, for Ar and Xe 20 and more extra LOs are necessary. It is rather clear that the standard LAPW setup, i.e., without any NMR LOs would result in NMR shieldings that are several

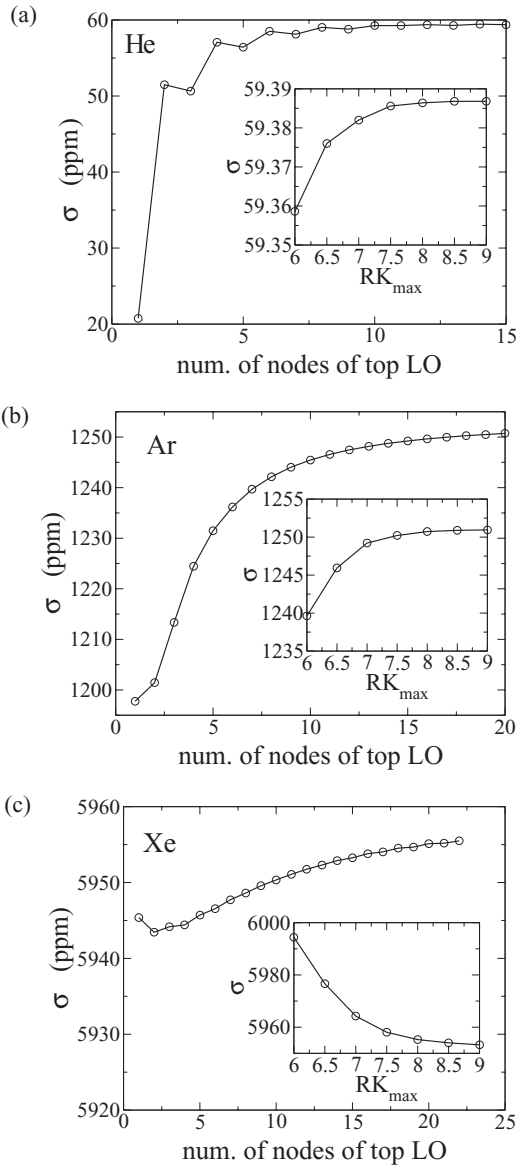


FIG. 4. The convergence of the absolute NMR shifts evaluated with respect to the number of NMR LOs, or equivalently, to the number of nodes of the highest LO in the configuration. In all three cases, the LOs have been added only for the  $s$ ,  $p$ , and  $d$  character (the  $4f$  states of Xe are in the core). The insets show the convergence with respect to the LAPW basis size, which is expressed using the product  $RK_{\max}$ , where  $R$  is a radius of the smallest atomic sphere and  $K_{\max}$  is the plane-wave cutoff.

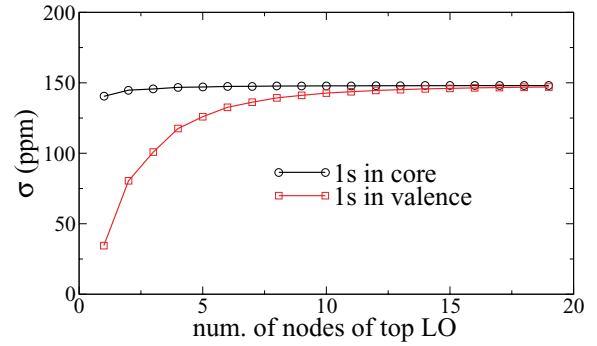


FIG. 5. (Color online) The convergence of the NMR shifts with respect to the number of NMR LOs evaluated for the Be atom with the  $1s$  states treated as core or valence state, respectively.

ppm off from convergence. Furthermore, in these particular cases, the shifts calculated from Eq. (62) are equal to 59.7 for He, 1245.8 for Ar, and 5952.5 for Xe. The numbers calculated with perturbation theory are 59.4 for He, 1250.6 for Ar, and 5954.5. Considering the errors introduced by the finite size of the supercell and the differences in the radial functions used in the perturbative calculations, the agreement is very good. The insets in Fig. 4 display the convergence of the NMR shifts with respect to the number of augmented plane waves. The basis set quality in the LAPW method is traditionally expressed by the product  $RK_{\max}$ , where  $R$  is the radius of the smallest atomic sphere and  $K_{\max}$  is the plane-wave cutoff.  $RK_{\max}$  equal to 7 is the default WIEN2k value, which is a good compromise between quality and performance for most quantities. As we can see, the NMR shifts are not much more demanding in this context.

Another issue we would like to mention here is the dependence of the convergence rate of the NMR LOs on the localization of the corresponding valence orbitals. To illustrate this, we calculate the NMR shifts for the Be atom, where we treat the  $1s$  state either as core or valence state. The results are displayed in Fig. 5. The converged value of the NMR shift [148.14 ppm from perturbation theory versus 148.08 ppm calculated from Eq. (62)] does not depend on how we treat the  $1s$  state, but the convergence rate with respect to the NMR-LO basis set is much faster when this state is excluded from the valence panel. This effect is directly related to the fact that the first-order perturbation of the deep and localized states are much more difficult to represent using our basis. In Fig. 3, we may notice that all radial functions have a relatively similar behavior around the nucleus. The radial functions are always solutions of the radial Schrödinger (Dirac) equation in a spherical potential, therefore they behave like  $r^l$  for small  $r$ . As a consequence, we need to add NMR LOs with relatively large numbers of nodes in order to properly expand the perturbation of the deep (core) states. A similar experience was made by Friedrich *et al.*<sup>40</sup> in  $GW$  calculations of ZnO using the LAPW method. Also there, they had to use a large number of local orbitals to increase the flexibility of the basis.

## B. Comparison with GIPAW

In order to further validate our implementation, we compare calculated isotropic shifts with the results obtained using

TABLE II. The isotropic shielding for various nuclei and compounds calculated with the LAPW method and the corresponding GIPAW results from literature.

	core	LAPW	GIPAW
H atom			
LiH		26.9	26.3 <sup>a</sup>
CH <sub>4</sub>		31.0	30.9 <sup>b</sup>
SiH <sub>4</sub>		26.7	27.3 <sup>b</sup>
C <sub>6</sub> H <sub>6</sub>		22.9	22.7 <sup>b</sup>
C atom			
diamond	200.5	142.0	133.1 <sup>b</sup>
CH <sub>4</sub>	200.5	194.4	191.0 <sup>b</sup>
CF <sub>4</sub>	199.1	38.0	34.2 <sup>b</sup>
C <sub>6</sub> H <sub>6</sub>	199.0	41.4	36.1 <sup>b</sup>
O atom			
	1s		
BeO	271.1	243.3	229.9 <sup>c</sup>
BaO	271.1	-455.6	-444.2 <sup>c</sup>
SrO	270.7	-200.4	-205.2 <sup>c</sup>
MgO	271.1	204.5	198.0 <sup>c</sup>
SrTiO <sub>3</sub>	271.1	-272.9	-301.3 <sup>c</sup>
F atom			
	1s		
LiF	306.4	383.0	369.3 <sup>d</sup>
NaF	306.5	406.3	395.8 <sup>d</sup>
MgF <sub>2</sub>	306.4	374.7	362.7 <sup>d</sup>
KF	305.4	283.3	268.1 <sup>d</sup>
CaF <sub>2</sub>	305.8	233.9	220.0 <sup>d</sup>
RbF	306.3	236.6	221.3 <sup>d</sup>
SrF <sub>2</sub>	305.8	229.3	215.3 <sup>d</sup>
CsF	306.4	142.6	136.3 <sup>d</sup>
BaF <sub>2</sub>	306.6	142.5	151.9 <sup>d</sup>
Si atom			
	1s2s2p		
SiH <sub>4</sub>	835.3	426.6	428.0 <sup>b</sup>
SiF <sub>4</sub>	835.5	411.3	410.0 <sup>b</sup>

<sup>a</sup>Reference 6.

<sup>b</sup>Reference 8.

<sup>c</sup>Reference 23.

<sup>d</sup>Reference 22.

the GIPAW approach. Table II and Fig. 6 summarize the comparison. The chemical shifts of H, C, and Si are compared with Ref. 8 and, consequently, the local density approximation (LDA) was used. The molecules were treated using a big supercell with a volume of 6000 Bohr<sup>3</sup>. The calculations for fluorides and oxides were performed with the PBE exchange-correlation<sup>41</sup> functional. The structural parameters and GIPAW results for fluorides have been taken from Ref. 22. In the case of oxides, we follow Ref. 23 and optimize the structural parameters. The NMR shifts converge relatively fast with the number of augmented plane waves, see for instance the insets in Fig. 4. For all solids investigated in this work,  $R_{\min}K_{\max}$  equal 8 was used to determine the size of the augmented-plane-wave basis set. For molecules, however, with the small atomic spheres for the H atom,  $R_{\min}K_{\max}$  equal to 3.5 is sufficient. In these cases, the atomic sphere radii of Si and C are at least two times larger than for the hydrogen atom, therefore the effective  $RK_{\max}$  for these atoms is of course much larger. The basis set for all systems has been constructed using many NMR LOs with up to 20 more nodes than the

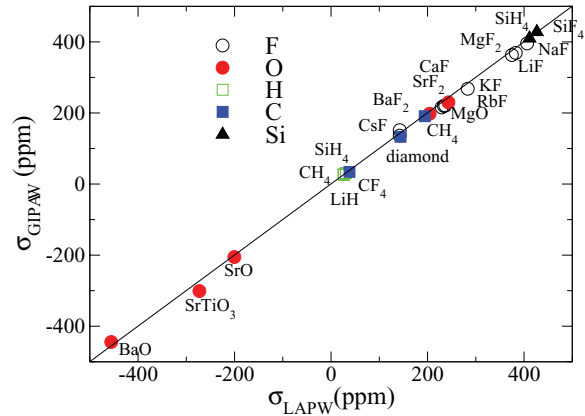


FIG. 6. (Color online) Comparison of the isotropic shielding calculated using our LAPW implementation and GIPAW from Refs. 6,8,22 and 23.

number of nodes of the corresponding valence wave function. This leads to results converged within 0.1 ppm. In order to test the sensitivity of the results with respect to the atomic sphere radii, we changed them by up to 20%, but the results changed only within a fraction of ppm. The  $k$  space integration has been done using uniform and shifted  $k$  meshes with a distance between  $k$  points close to 0.015 Bohr<sup>-1</sup>. For molecules, we use only the  $\Gamma$  point.

We compare the absolute NMR shifts calculated with the LAPW and the GIPAW method in Table II. Clearly, the agreement depends on the specific element. For hydrogen, the discrepancy is less than 1 ppm, for Si, it stays within 2 ppm, for carbon, it increases to 5 ppm, except for diamond, where it is nearly 9 ppm. For oxides and fluorides, the differences between LAPW and GIPAW can be as big as 20 ppm, but since the chemical shifts vary in a range of  $\pm 400$  ppm, even in those cases the overall trends are quite well represented by both methods as shown in Fig. 6. The core states are evaluated using the SCF converged potential, therefore the core contribution to the total NMR chemical shift of a particular nucleus is not constant. However, for present examples, it varies less than 2 ppm.

#### IV. CONCLUSIONS

We have presented a method for the calculation of NMR chemical shifts within the all-electron APW method. Our implementation is based on density functional perturbation theory. We follow the GIPAW method,<sup>8</sup> except where obvious differences result from the different bases sets in these methods. In particular, we had to resolve two main issues, namely, the integration of the current according to Biot-Savart's law, which cannot be performed in reciprocal space only (as in GIPAW), but due to the all-electron character of our induced current, we had to develop an integration procedure based on Weinert's pseudocharge method. The second issue is related to the missing flexibility of the standard LAPW basis set for representing the first-order perturbation of the occupied orbitals. The LAPW basis set is very accurate for states with eigenvalues close to the linearization energies, which covers usually the valence and the lowest conduction bands. In order

to provide sufficient flexibility to represent the perturbed wave functions, we had to add extra basis functions in the form of local orbitals. The linearization energies of those NMR LOs are set such that the radial functions have a node at the sphere boundary and the number of nodes inside the sphere increases for subsequent LOs.

The perturbative approach is checked to reproduce the diamagnetic response of isolated spherical atoms, which can be computed accurately by a much simpler approach. To further benchmark our implementation, we compared our results with the GIPAW results from literature for several solids and molecules. Overall the NMR chemical shifts agree quite well with the literature values, although in a few cases, differences as large as 20 ppm are present.

### ACKNOWLEDGMENTS

We acknowledge support from the Austrian Science Fund (FWF) for project SFB-F41 (ViCoM) and fruitful discussions and advice by J. Yates.

### APPENDIX A: DERIVATIVES OF THE SPHERICAL HARMONICS

In the LAPW method, the wave functions inside the atomic spheres are represented as products of radial wave functions times spherical harmonics  $[W_{lm}(r)Y_{lm}(\hat{\mathbf{r}})]$ . Due to the presence of the momentum operator, we have to calculate derivatives of these products in the Cartesian reference frame. The derivatives are expressed using operators in the spherical frame of reference:

$$\begin{aligned}\frac{\partial}{\partial x} &= \frac{1}{\sqrt{2}}(\nabla_{-1} - \nabla_{+1}), \\ \frac{\partial}{\partial y} &= \frac{i}{\sqrt{2}}(\nabla_{-1} + \nabla_{+1}), \\ \frac{\partial}{\partial z} &= \nabla_0.\end{aligned}\quad (\text{A1})$$

The derivatives  $\nabla_{-1}$ ,  $\nabla_0$  and  $\nabla_{+1}$  of  $W_{lm}(r)Y_{lm}(\hat{\mathbf{r}})$  are expressed as follows:

$$\begin{aligned}\nabla_0[W(r)Y_{lm}(\hat{\mathbf{r}})] &= F_+^0(lm)W_+(r)Y_{l+1,m} \\ &+ F_-^0(lm)W_-(r)Y_{l-1,m},\end{aligned}$$

$$\begin{aligned}\nabla_{\pm 1}[W(r)Y_{lm}(\hat{\mathbf{r}})] &= F_{\pm}^{\pm 1}(lm)W_+(r)Y_{l+1,m\pm 1} \\ &+ F_{\pm}^{\pm 1}(lm)W_-(r)Y_{l-1,m\pm 1},\end{aligned}$$

where  $W_1(r)$  and  $W_2(r)$  are

$$W_+(r) = \frac{\partial}{\partial r}W(r) - \frac{l}{r}W(r), \quad (\text{A2})$$

$$W_-(r) = \frac{\partial}{\partial r}W(r) + \frac{l+1}{r}W(r), \quad (\text{A3})$$

and  $F_{\pm}^{0,\pm}(lm)$  are expressed as

$$F_+^0(lm) = \sqrt{\frac{(l+m+1)(l-m+1)}{(2l+1)(2l+3)}}, \quad (\text{A4})$$

$$F_-^0(lm) = \sqrt{\frac{(l+m)(l-m)}{(2l-1)(2l+1)}}, \quad (\text{A5})$$

$$F_+^{\pm 1}(lm) = \sqrt{\frac{(l \pm m + 1)(l \pm m + 2)}{2(2l+1)(2l+3)}}, \quad (\text{A6})$$

$$F_-^{\pm 1}(lm) = -\sqrt{\frac{(l \mp m - 1)(l \mp m)}{2(2l-1)(2l+1)}}. \quad (\text{A7})$$

### APPENDIX B: CURRENT DENSITY INSIDE THE SPHERES

If we write the current density inside the spheres as

$$\mathbf{j}_{\text{ind}}(\mathbf{r}) = \text{Re} \left[ \sum_{LM} \mathbf{j}_{LM}^{\alpha}(r) Y_{LM} \right], \quad (\text{B1})$$

the  $\mathbf{j}_{lm}^{\alpha}(r)$  components are then evaluated using following limit:

$$\mathbf{j}_{LM}^{\alpha}(r) = \lim_{q \rightarrow 0} \frac{1}{2q} [\mathbf{S}_{LM}(r, q) - \mathbf{S}_{LM}(r, -q)], \quad (\text{B2})$$

where the  $\mathbf{S}_{LM}(r, q)$  are given by

$$\mathbf{S}_{LM}(r, q) = \frac{1}{cN_{\mathbf{k}}} \sum_{\alpha=x,y,z} \sum_{\mathbf{k},o} \{ [\mathbf{A}_{\mathbf{k},q_{\alpha}}^o(r)]_{LM} + [\mathbf{B}_{\mathbf{k},q_{\alpha}}^o(r)]_{LM} \}, \quad (\text{B3})$$

The Cartesian coordinates of the vector  $[\mathbf{A}_{\mathbf{k},q_{\alpha}}^o(r)]_{LM}$  can be evaluated using the following formulas:

$$[A_{x,\mathbf{k},\mathbf{q}}^o(r)]_{LM} = \sqrt{\frac{\pi}{3}} e^{-i\mathbf{q}\cdot\mathbf{r}_a} \{ [A_{-1,\mathbf{k},\mathbf{q}}^o(r)]_{LM}^+ + [A_{-1,\mathbf{k},\mathbf{q}}^o(r)]_{LM}^- - [A_{+1,\mathbf{k},\mathbf{q}}^o(r)]_{LM}^+ - [A_{+1,\mathbf{k},\mathbf{q}}^o(r)]_{LM}^- \}, \quad (\text{B4})$$

$$[A_{y,\mathbf{k},\mathbf{q}}^o(r)]_{LM} = i\sqrt{\frac{\pi}{3}} e^{-i\mathbf{q}\cdot\mathbf{r}_a} \{ [A_{-1,\mathbf{k},\mathbf{q}}^o(r)]_{LM}^+ + [A_{-1,\mathbf{k},\mathbf{q}}^o(r)]_{LM}^- + [A_{+1,\mathbf{k},\mathbf{q}}^o(r)]_{LM}^+ + [A_{+1,\mathbf{k},\mathbf{q}}^o(r)]_{LM}^- \}, \quad (\text{B5})$$

$$[A_{z,\mathbf{k},\mathbf{q}}^o(r)]_{LM} = \sqrt{\frac{2\pi}{3}} e^{-i\mathbf{q}\cdot\mathbf{r}_a} \{ [A_{0,\mathbf{k},\mathbf{q}}^o(r)]_{LM}^+ + [A_{0,\mathbf{k},\mathbf{q}}^o(r)]_{LM}^- \}, \quad (\text{B6})$$

where  $[A_{\pm 1,\mathbf{k},\mathbf{q}}^o(r)]_{LM}^{\pm}$  and  $[A_{0,\mathbf{k},\mathbf{q}}^o(r)]_{LM}^{\pm}$  are given by

$$\begin{aligned}[A_{-1,\mathbf{k},\mathbf{q}}^o(r)]_{LM}^{\pm} &= \sum_{lm} \sum_{l'm'} \sum_{L'M'} R_{lm,l'm'}^{\circ,\pm}(r) [\sqrt{6} G_{l\pm 1 l' L'}^{m' M' 0} G_{l\pm 1 l' L'}^{m-1 M' M} + i(q_x - iq_y) G_{l' L' 1}^{m' M' 1} G_{l\pm 1 l' L'}^{m-1 M' M} \\ &- i(q_x + iq_y) G_{l' L' 1}^{m' M' 0} G_{l\pm 1 l' L'}^{m-1 M' M} - i(\sqrt{2}) q_z G_{l' L' 1}^{m' M' -1} G_{l\pm 1 l' L'}^{m-1 M' M}] F_{\pm}^{-1}(lm),\end{aligned}$$

$$\begin{aligned}
[A_{\pm 1, \mathbf{k}, \mathbf{q}}^o(r)]_{LM}^{\pm} &= \sum_{lm} \sum_{l'm'} \sum_{L'M'} R_{lm, l'm'}^{o, \pm}(r) [\sqrt{6} G_{l\pm 1L'L'}^{m'M'0} G_{l\pm 1L'L'}^{m+1M'M} + i(q_x - iq_y) G_{l'L'L'}^{m'M'1} G_{l\pm 1L'L'}^{m+1M'M} \\
&\quad - i(q_x + iq_y) G_{l'L'L'}^{m'M'0} G_{l\pm 1L'L'}^{m+1M'M} - i(\sqrt{2}) q_z G_{l'L'L'}^{m'M'-1} G_{l\pm 1L'L'}^{m+1M'M}] F_{\pm}^{\pm}(lm), \\
[A_{0, \mathbf{k}, \mathbf{q}}^o(r)]_{LM}^{\pm} &= \sum_{lm} \sum_{l'm'} \sum_{L'M'} R_{lm, l'm'}^{o, \pm}(r) [\sqrt{6} G_{l\pm 1L'L'}^{m'M'0} G_{l\pm 1L'L'}^{mM'M} + i(q_x - iq_y) G_{l'L'L'}^{m'M'1} G_{l\pm 1L'L'}^{mM'M} \\
&\quad - i(q_x + iq_y) G_{l'L'L'}^{m'M'0} G_{l\pm 1L'L'}^{mM'M} - i(\sqrt{2}) q_z G_{l'L'L'}^{m'M'-1} G_{l\pm 1L'L'}^{mM'M}] F_{\pm}^0(lm),
\end{aligned}$$

where  $R_{lm, l'm'}^{o, \pm}(r) = r W_{\pm, lm}^{o, \mathbf{k}}(r) W_{l'm'}^{(1), o, \mathbf{k}+\mathbf{q}}(r)$  and  $F_{\pm}^0(lm)$  are defined in the Appendix A.  $W_{\pm, lm}^{o, \mathbf{k}}(r)$  and  $W_{l'm'}^{(1), o, \mathbf{k}+\mathbf{q}}(r)$  are the radial functions entering the spherical harmonic expansion of the wave function [see Eq. (25)] of occupied states and their first-order perturbation. Similarly, the expressions for the components of the  $[\mathbf{B}_{\mathbf{k}, \mathbf{q}}^o(r)]_{LM}$  vector are

$$[B_{x, \mathbf{k}, \mathbf{q}}^o(r)]_{LM} = \sqrt{\frac{\pi}{3}} e^{-i\mathbf{q}\cdot\mathbf{r}_a} \{ [B_{-1, \mathbf{k}, \mathbf{q}}^o(r)]_{LM}^+ + [B_{-1, \mathbf{k}, \mathbf{q}}^o(r)]_{LM}^- - [B_{+1, \mathbf{k}, \mathbf{q}}^o(r)]_{LM}^+ - [B_{+1, \mathbf{k}, \mathbf{q}}^o(r)]_{LM}^- \}, \quad (\text{B7})$$

$$[B_{y, \mathbf{k}, \mathbf{q}}^o(r)]_{LM} = i\sqrt{\frac{\pi}{3}} e^{-i\mathbf{q}\cdot\mathbf{r}_a} \{ [B_{-1, \mathbf{k}, \mathbf{q}}^o(r)]_{LM}^+ + [B_{-1, \mathbf{k}, \mathbf{q}}^o(r)]_{LM}^- + [B_{+1, \mathbf{k}, \mathbf{q}}^o(r)]_{LM}^+ + [B_{+1, \mathbf{k}, \mathbf{q}}^o(r)]_{LM}^- \}, \quad (\text{B8})$$

$$[B_{z, \mathbf{k}, \mathbf{q}}^o(r)]_{LM} = \sqrt{\frac{2\pi}{3}} e^{-i\mathbf{q}\cdot\mathbf{r}_a} \{ [B_{0, \mathbf{k}, \mathbf{q}}^o(r)]_{LM}^+ + [B_{0, \mathbf{k}, \mathbf{q}}^o(r)]_{LM}^- \}, \quad (\text{B9})$$

with  $[B_{\pm 1, \mathbf{k}, \mathbf{q}}^o(r)]_{LM}^{\pm}$  and  $[B_{0, \mathbf{k}, \mathbf{q}}^o(r)]_{LM}^{\pm}$  given by

$$\begin{aligned}
[B_{-1, \mathbf{k}, \mathbf{q}}^o(r)]_{LM}^{\pm} &= \sum_{lm} \sum_{l'm'} \sum_{L'M'} R_{lm, l'm'}^{o, \pm}(r) [\sqrt{6} G_{l\pm 1L'L'}^{m'-1M'0} G_{lL'L'}^{mM'M} + i(q_x - iq_y) G_{l\pm 1L'L'}^{m'-1M'1} G_{lL'L'}^{mM'M} \\
&\quad - i(q_x + iq_y) G_{l\pm 1L'L'}^{m'-1M'0} G_{lL'L'}^{mM'M} - i(\sqrt{2}) q_z G_{l\pm 1L'L'}^{m'-1M'-1} G_{lL'L'}^{mM'M}] F_{\pm}^{-1}(lm), \\
[B_{+1, \mathbf{k}, \mathbf{q}}^o(r)]_{LM}^{\pm} &= \sum_{lm} \sum_{l'm'} \sum_{L'M'} R_{lm, l'm'}^{o, \pm}(r) [\sqrt{6} G_{l\pm 1L'L'}^{m'+1M'0} G_{lL'L'}^{mM'M} + i(q_x - iq_y) G_{l\pm 1L'L'}^{m'+1M'1} G_{lL'L'}^{mM'M} \\
&\quad - i(q_x + iq_y) G_{l\pm 1L'L'}^{m'+1M'0} G_{lL'L'}^{mM'M} - i(\sqrt{2}) q_z G_{l\pm 1L'L'}^{m'+1M'-1} G_{lL'L'}^{mM'M}] F_{\pm}^{+1}(lm), \\
[B_{0, \mathbf{k}, \mathbf{q}}^o(r)]_{LM}^{\pm} &= \sum_{lm} \sum_{l'm'} \sum_{L'M'} R_{lm, l'm'}^{o, \pm}(r) [\sqrt{6} G_{l\pm 1L'L'}^{m'M'0} G_{lL'L'}^{mM'M} + i(q_x - iq_y) G_{l\pm 1L'L'}^{m'M'1} G_{lL'L'}^{mM'M} \\
&\quad - i(q_x + iq_y) G_{l\pm 1L'L'}^{m'M'0} G_{lL'L'}^{mM'M} - i\sqrt{2} q_z G_{l\pm 1L'L'}^{m'M'-1} G_{lL'L'}^{mM'M}] F_{\pm}^0(lm).
\end{aligned}$$

The evaluation of the first-order perturbation  $|\Psi_{o, \mathbf{k}, \mathbf{q}_a}^{(1)}\rangle$  requires the matrix elements  $\mathbf{C}_{\mathbf{k}, \mathbf{q}_a}^o$  [see Eq. (36)]. The expressions for the sphere part of the integrals are similar to the formulas for the  $\mathbf{B}_{\mathbf{k}, \mathbf{q}_a}^o(\mathbf{r}')$  vectors. However, in this case, the momentum operator acts on the wave functions of the occupied states  $|\Psi_{o, \mathbf{k}}\rangle$ , the modulating function is  $e^{i\mathbf{q}\cdot\mathbf{r}'}$  and the expression is integrated over  $\mathbf{r}'$ . The integrals  $\mathbf{C}_{\mathbf{k}, \mathbf{q}_a}^o$  are evaluated using the following formulas:

$$\mathbf{C}_{\mathbf{k}, \mathbf{q}}^o = (\mathbf{B} \times \alpha) \cdot [C_{x, \mathbf{k}, \mathbf{q}}^o, C_{y, \mathbf{k}, \mathbf{q}}^o, C_{z, \mathbf{k}, \mathbf{q}}^o], \quad (\text{B10})$$

$$C_{x, \mathbf{k}, \mathbf{q}}^o = e^{i\mathbf{q}\cdot\mathbf{r}_a} \sqrt{2\pi} [(C_{-1, \mathbf{k}, \mathbf{q}}^o)^+ + (C_{-1, \mathbf{k}, \mathbf{q}}^o)^- - (C_{+1, \mathbf{k}, \mathbf{q}}^o)^+ - (C_{+1, \mathbf{k}, \mathbf{q}}^o)^-], \quad (\text{B11})$$

$$C_{y, \mathbf{k}, \mathbf{q}}^o = e^{i\mathbf{q}\cdot\mathbf{r}_a} i\sqrt{2\pi} [(C_{-1, \mathbf{k}, \mathbf{q}}^o)^+ + (C_{-1, \mathbf{k}, \mathbf{q}}^o)^- + (C_{+1, \mathbf{k}, \mathbf{q}}^o)^+ + (C_{+1, \mathbf{k}, \mathbf{q}}^o)^-], \quad (\text{B12})$$

$$C_{z, \mathbf{k}, \mathbf{q}}^o = e^{i\mathbf{q}\cdot\mathbf{r}_a} \sqrt{4\pi} [(C_{0, \mathbf{k}, \mathbf{q}}^o)^+ + (C_{0, \mathbf{k}, \mathbf{q}}^o)^-], \quad (\text{B13})$$

with  $[C_{\pm 1, \mathbf{k}, \mathbf{q}}^o(r)]_{LM}^{\pm}$  and  $[C_{0, \mathbf{k}, \mathbf{q}}^o(r)]_{LM}^{\pm}$  given by

$$\begin{aligned}
(C_{-1, \mathbf{k}, \mathbf{q}}^o)^{\pm} &= \sum_{lm} \sum_{l'm'} \sum_{L'M'} \sqrt{\frac{2\pi}{3}} I_{lm, l'm'}^{o, \pm} [\sqrt{6} G_{l\pm 1L'L'}^{m'-1M'0} + i(-q_x + iq_y) G_{l\pm 1L'L'}^{m'-1M'1} \\
&\quad + i(q_x + iq_y) G_{l\pm 1L'L'}^{m'-1M'0} + i(\sqrt{2}) q_z G_{l\pm 1L'L'}^{m'-1M'-1}] G_{lL'L'}^{mM'M} F_{\pm}^{-1}(lm),
\end{aligned}$$

$$\begin{aligned}
(C_{+1, \mathbf{k}, \mathbf{q}}^o)^{\pm} &= \sum_{lm} \sum_{l'm'} \sum_{L'M'} \sqrt{\frac{2\pi}{3}} I_{lm, l'm'}^{o, \pm} [\sqrt{6} G_{l\pm 1L'L'}^{m'+1M'0} + i(-q_x + iq_y) G_{l\pm 1L'L'}^{m'+1M'1} \\
&\quad + i(q_x + iq_y) G_{l\pm 1L'L'}^{m'+1M'0} + i(\sqrt{2}) q_z G_{l\pm 1L'L'}^{m'+1M'-1}] G_{lL'L'}^{mM'M} F_{\pm}^{+1}(lm),
\end{aligned}$$

$$(C_{z,\mathbf{k},\mathbf{q}}^o)^\pm = \sum_{lm} \sum_{l'm'} \sum_{L'M'} \sqrt{\frac{2\pi}{3}} I_{lm,l'm'}^{o,\pm} [\sqrt{6} G_{l'\pm 1L'0}^{m'M'0} + i(-q_x + iq_y) G_{l'\pm 1L'1}^{m'M'1} \\ + i(q_x + iq_y) G_{l'\pm 1L'1}^{m'M'0} + i\sqrt{2} q_z G_{l'\pm 1L'1}^{m'M'-1}] G_{lL'0}^{mM'0} F_\pm^0(lm),$$

where  $I_{lm,l'm'}^{o,\pm} = \int_0^{R_{MT}} dr r W_{\pm,l',m'}^{o,\mathbf{k}}(r) W_{lm}^{\alpha,\mathbf{k}+\mathbf{q}}(r)$  and  $\alpha$  stands for either occupied or empty states depending on the method used for computing  $|\Psi_{o,\mathbf{k}+\mathbf{q}_\alpha}^{(1)}\rangle$ . Similarly to  $\mathbf{A}^o$  and  $\mathbf{B}^o$ , the interstitial part of the integral is easily calculated using Eq. (36) and including a Fourier transform of the step function.

- 
- <sup>1</sup> *Encyclopedia of NMR*, edited by C. M. Grant and R. K. Harris (Wiley, New York, 1996).
- <sup>2</sup> M. Schindler, *J. Am. Chem. Soc.* **109**, 1020 (1987).
- <sup>3</sup> A. Zheng, S.-B. Liu, and F. Deng, *J. Phys. Chem. C* **113**, 15018 (2009).
- <sup>4</sup> T. Helgaker, M. Jaszunski, and K. Ruud, *Chem. Rev.* **99**, 293 (1999).
- <sup>5</sup> *Calculation of NMR and EPR Parameters: Theory and Applications*, edited by M. Kaupp, M. Bühl, and V. G. Malkin (Wiley, New York, 2004).
- <sup>6</sup> F. Mauri, B. G. Pfrommer, and S. G. Louie, *Phys. Rev. Lett.* **77**, 5300 (1996).
- <sup>7</sup> D. Sebastiani and M. Parrinello, *J. Phys. Chem. A* **105**, 1951 (2001).
- <sup>8</sup> C. J. Pickard and F. Mauri, *Phys. Rev. B* **63**, 245101 (2001).
- <sup>9</sup> T. Thonhauser, D. Ceresoli, A. A. Mostofi, N. Marzari, R. Resta, and D. Vanderbilt, *J. Chem. Phys.* **131**, 101101 (2009).
- <sup>10</sup> D. Skachkov, M. Krykunov, and T. Ziegler, *Can. J. Chem.* **89**, 1150 (2011).
- <sup>11</sup> P. Hohenberg and W. Kohn, *Phys. Rev. B* **136**, 864 (1964).
- <sup>12</sup> W. Kohn and L. J. Sham, *Phys. Rev. A* **140**, 1133 (1965).
- <sup>13</sup> T. Gregor, F. Mauri, and R. Car, *J. Chem. Phys.* **111**, 1815 (1999).
- <sup>14</sup> F. Mauri, B. G. Pfrommer, and S. G. Louie, *Phys. Rev. Lett.* **79**, 2340 (1997).
- <sup>15</sup> Y.-G. Yoon, B. G. Pfrommer, F. Mauri, and S. G. Louie, *Phys. Rev. Lett.* **80**, 3388 (1998).
- <sup>16</sup> F. Mauri, B. G. Pfrommer, and S. G. Louie, *Phys. Rev. B* **60**, 2941 (1999).
- <sup>17</sup> F. Mauri, A. Pasquarello, B. G. Pfrommer, Y.-G. Yoon, and S. G. Louie, *Phys. Rev. B* **62**, R4786 (2000).
- <sup>18</sup> F. Buda, P. Giannozzi, and F. Mauri, *J. Phys. Chem. B* **104**, 9048 (2000).
- <sup>19</sup> B. G. Pfrommer, F. Mauri, and S. G. Louie, *J. Am. Chem. Soc.* **122**, 123 (2000).
- <sup>20</sup> P. E. Blöchl, *Phys. Rev. B* **50**, 17953 (1994).
- <sup>21</sup> J. R. Yates, C. J. Pickard, and F. Mauri, *Phys. Rev. B* **76**, 024401 (2007).
- <sup>22</sup> A. Sadoc, M. Body, C. Legein, M. Biswal, F. Fayon, X. Rocquefelte, and F. Boucher, *Phys. Chem. Chem. Phys.* **13**, 18539 (2011).
- <sup>23</sup> D. S. Middlemiss, F. Blanc, C. J. Pickard, and C. P. Grey, *J. Magn. Reson.* **204**, 1 (2010).
- <sup>24</sup> S. E. Ashbrook, L. Le Polles, R. Gautier, C. J. Pickard, and R. I. Walton, *Phys. Chem. Chem. Phys.* **8**, 3423 (2006).
- <sup>25</sup> J. M. Griffin, J. R. Yates, A. J. Berry, S. Wimperis, and S. E. Ashbrook, *J. Am. Chem. Soc.* **132**, 15651 (2010).
- <sup>26</sup> M. Profeta, F. Mauri, and C. J. Pickard, *J. Am. Chem. Soc.* **125**, 541 (2003).
- <sup>27</sup> A.-C. Uldry *et al.*, *J. Am. Chem. Soc.* **130**, 945 (2008).
- <sup>28</sup> J.-S. Filhol, J. Deschamps, S. G. Dutremez, B. Boury, T. Barisien, L. Legrand, and M. Schott, *J. Am. Chem. Soc.* **131**, 6976 (2009).
- <sup>29</sup> R. K. Harris, S. Cadars, L. Emsley, J. R. Yates, C. J. Pickard, R. K. R. Jetti, and U. J. Griesser, *Phys. Chem. Chem. Phys.* **9**, 360 (2007).
- <sup>30</sup> URL <http://www.gipaw.net>.
- <sup>31</sup> S. Piana, D. Sebastiani, P. Carloni, and M. Parrinello, *J. Am. Chem. Soc.* **123**, 8730 (2001).
- <sup>32</sup> V. Weber, M. Iannuzzi, S. Giani, J. Hutter, R. Declerck, and M. Waroquier, *J. Chem. Phys.* **131**, 014106 (2009).
- <sup>33</sup> G. Lippert, J. Hutter, and M. Parrinello, *Theor. Chem. Acc.* **103**, 124 (1999).
- <sup>34</sup> D. Ceresoli, N. Marzari, M. G. Lopez, and T. Thonhauser, *Phys. Rev. B* **81**, 184424 (2010).
- <sup>35</sup> D. J. Singh and L. Nordström, *Planewaves, Pseudopotentials and the LAPW Method*, 2nd ed. (Springer, New York, 2006).
- <sup>36</sup> P. Blaha, K. Schwarz, G. K. H. Madsen, D. Kvasnicka, and J. Luitz, *WIEN2k, An Augmented Plane Wave Plus Local Orbitals Program for Calculating Crystal Properties*, Vienna University of Technology, Austria (2001).
- <sup>37</sup> E. Sjöstedt, L. Nordström, and D. J. Singh, *Solid State Commun.* **114**, 15 (2000).
- <sup>38</sup> G. K. H. Madsen, P. Blaha, K. Schwarz, E. Sjöstedt, and L. Nordström, *Phys. Rev. B* **64**, 195134 (2001).
- <sup>39</sup> M. Weinert, *J. Math. Phys.* **22**, 11 (1981).
- <sup>40</sup> C. Friedrich, M. C. Müller, and S. Blügel, *Phys. Rev. B* **83**, 081101 (2011).
- <sup>41</sup> J. P. Perdew, K. Burke, and M. Ernzerhof, *Phys. Rev. Lett.* **77**, 3865 (1996).